Bioorganic Chemistry 92 (2019) 103186

Contents lists available at ScienceDirect

Bioorganic Chemistry

journal homepage: www.elsevier.com/locate/bioorg

Physapubescin I from husk tomato suppresses SW1990 cancer cell growth by targeting kidney-type glutaminase

Kai-Yin Yang[a,1], Can-Rong Wu[a,1], Meng-Zhu Zheng[a,1], Ruo-Tian Tang[a], Xing-Zhou Li[c,*], Li-Xia Chen[b,*], Hua Li[a,b,*]

[a] Hubei Key Laboratory of Natural Medicinal Chemistry and Resource Evaluation, School of Pharmacy, Tongji Medical College, Huazhong University of Science and Technology, Wuhan 430030, China
[b] Wuya College of Innovation, Key Laboratory of Structure-Based Drug Design & Discovery, Ministry of Education, Shenyang Pharmaceutical University, Shenyang 110016, China
[c] National Engineering Research Center for the Emergency Drug, Beijing Institute of Pharmacology and Toxicology, Beijing 100850, China

ARTICLE INFO

Keywords:
KGA
Physapubescin I
Inhibitor
Cancer therapy

ABSTRACT

Kidney-type glutaminase (KGA), catalyzing the hydrolysis of glutamine to glutamate for energy supply, is over-expressed in many cancers and has been regarded as a new therapeutic target for cancers. Physapubescin I was isolated from the fruits of the edible herb *Physalis pubescens* L., commonly named as "husk tomato or hairy groundcherry", and was predicted to be a potential KGA inhibitor through structure-based virtual ligand screening. Enzyme inhibition assays, microscale thermophoresis (MST) and cellular thermal shift assay (CETSA) experiments have demonstrated the high efficiency and specificity of physapubescin I targeting KGA. EdU proliferation, Hoechst 33258 staining and cytotoxicity assays indicated that physapubescin I could inhibit cancer cell proliferation and promote apoptosis more effectively than the known KGA inhibitor, BPTES. Knockdown of KGA by siRNA reduced the inhibition of physapubescin I to SW1990 cells. Meanwhile, physapubescin I impaired glutamine metabolism in SW1990 cells with increasing intracellular level of glutamine, and correspondingly decreasing glutamate and its downstream metabolites, which may account for its inhibition of cancer cell proliferation and proapoptosis. Physapubescin I also showed significant tumor growth inhibition and low toxicity in a SW1990 xenograft mouse model. Collectively, physapubescin I may serve as a potential drug candidate or lead compound for cancer therapy by targeting KGA.

1. Introduction

Glutaminase, the first enzyme in the glutaminolysis pathway, catalyzes the hydrolysis of glutamine to glutamate [1]. Glutamine serves as a precursor of a number of intermediates essential for biosynthetic pathways and energy production. Mammalian glutaminase exists in a variety of specific tissues and is encoded by two genes, kidney-type glutaminase (*GLS*) and liver-type glutaminase (*GLS2*). *GLS2* is mainly expressed in liver, brain, pituitary gland and pancreas with more complex roles in cancers. The role of *GLS2* as a tumor suppressor is controversial and further research and validation about the context-dependent role of *GLS2* in cancer is needed. *GLS* is more widely expressed in various tissues, which is considered to play a key role in various cancers [2–4]. Alternative splicing of *GLS* further increases its complexity. The pre-*GLS* transcript can be spliced into two isoforms of kidney-type glutaminase (KGA) or glutaminase C (GAC), while liver-type glutaminase (LGA) and a longer isoform glutaminase B (GAB) belong to *GLS2* [5].

Glutamine is an abundant and versatile nutrient, participating in energy formation, redox homeostasis, macromolecule synthesis and signaling in cancer cells. Carbon derived from glutamine can be used for anabolic biosynthesis by hydrolyzing glutamine to glutamate [6]. Although most tissues can synthesize glutamine during rapid growth or other stresses, when the demand exceeds the supply rate of cells, glutamine will become conditionally essential. This demand for glutamine is particularly important in cancer cells, so many of them exhibit

* Corresponding authors at: Hubei Key Laboratory of Natural Medicinal Chemistry and Resource Evaluation, School of Pharmacy, Tongji Medical College, Huazhong University of Science and Technology, Wuhan, 430030, China (H. Li); Wuya College of Innovation, Key Laboratory of Structure-Based Drug Design & Discovery, Ministry of Education, Shenyang Pharmaceutical University, Shenyang 110016, China (L.-X. Chen); National Engineering Research Center for the Emergency Drug, Beijing Institute of Pharmacology and Toxicology, Beijing 100850, China (X.-Z. Li).
E-mail addresses: xingzhouli@aliyun.com (X.-Z. Li), syzyclx@163.com (L.-X. Chen), li_hua@hust.edu.cn (H. Li).
[1] These authors contribute equally to this work.

https://doi.org/10.1016/j.bioorg.2019.103186
Received 23 January 2019; Received in revised form 31 July 2019; Accepted 5 August 2019
Available online 12 August 2019

oncogene-dependent glutamine addiction. This metabolic reprogramming usually depends on the activity of mitochondrial glutaminase [7,8]. It has been reported that some oncogenes including c-Myc, Raf, Ras and Rho GTpases could up-regulate KGA expression in many cancer cells [9–13]. Treating tumor cells with KGA specific siRNA induces apoptosis under oxidative stress [14]. Inhibition of KGA therefore has gained considerable attention as a new therapeutic approach for cancers [9,15–17].

Although KGA has been extensively studied as a key metabolic enzyme, only a few synthetic KGA inhibitors have been discovered so far, such as DON (6-diazo-5-oxo-L-norleucine), BPTES (bis-2-(5-phenylacetamido-1,2,4-thiadiazol-2-yl) ethyl sulfide), 968 (5-(3-bromo-4-(dimethylamino)phenyl)-2,2-dimethyl-2,3,5,6 tetrahydrobenzo[*a*]phenanthridin-4(1*H*)-one) and CB-839. CB-839 exhibited distinct synergistic anti-tumor activity when it was combined with paclitaxel to MDA-MB-231 orthotopic xenograft model or in combination with pomalidomide to multiple myeloma RPMI-8226 myeloma xenograft models. CB-839 is currently in clinical trials for several different indications. However, DON, as a traditional KGA inhibitor, lacks selectivity and has weak potency. BPTES, a KGA allosteric inhibitor, selectively inhibits KGA while study on BPTES has been terminated in the preclinical phase due to its poor metabolic stability and low solubility. 968 has no inhibitory effect against glutaminase which has been activated. This shortcoming and hydrophobicity limit the further application and continued research of 968 in the anti-tumor field [18–22]. The renewed interest in selective inhibition of KGA as a therapeutic approach has led to the continuous search for new inhibitors which are more potent and selective for KGA [23,24].

Physalis pubescens L. (Solanaceae), an edible and medical plant, produces nutritious and healthy fruits which commonly known as husk tomato or hairy groundcherry in English, and Gu-Niang in Chinese [25,26]. The fruits of *Physalis pubescens* are consumed as popular foods either fresh or processed, such as canning, jam or preserves. The calyces or whole plants of *Physalis pubescens* have also been used as traditional folk medicine for the treatment of sore throat, cough, and urogenital system diseases such as urethritis, hematuria, and orchitis in China [25,26]. This plant has been reported to be rich in withanolides, a group of naturally occurring C28 steroids with multiple bioactivities including antitumor, anti-inflammatory, immunosuppressive, and antimicrobial effects [27–29].

It is worth noting that natural products are considered to be a rich source for drug discovery and development [30]. In order to find highly potent and selective small-molecule KGA inhibitors from natural products, we screened over 100 compounds from *Physalis pubescens* including withanolides, flavonoids, and coumarins by a structure-based virtual ligand screening method. Fortunately, physapubescin I (Fig. 1A), a withanolide, was determined to target KGA with high efficiency and specificity for KGA enzyme. Moreover, it showed potent anticancer activity *in vitro* and inhibition of tumor cell growth *in vivo*.

2. Experimental

2.1. Compounds

The fresh fruits of *P. pubescens* L. (80 kg, collected from Shenyang, Liaoning Province, China) were cut into small pieces and extracted with EtOH/H_2O (75:25 v/v) (2 × 800 L). The resulting extract (3.6 kg) was concentrated in vacuum, suspended in H_2O (5.0 L), and partitioned successively with petroleum ether (PE) (3 × 5.0 L) and EtOAc (3 × 5.0 L) to give EtOAc fraction (350 g). It was subjected to a silica gel CC (12 × 100 cm) that was eluted with CH_2Cl_2/MeOH (100:1, 40:1, 20:1, 10:1, 4:1, 2:1, 1:1, and 0:1 v/v) to obtain nine combined subfractions (E1 − E10). Fraction E3 (42 g) was subjected to a silica gel CC (8 × 80 cm) and eluted with CH_2Cl_2/acetone (from 100:1 to 0:1 v/v) to produce five subfractions (E31 − E35). E33 (15.5 g) was chromatographed on a Sephadex LH-20 column (4.5 × 100 cm) eluted with CH_2Cl_2/MeOH (1:1 v/v) and further purified via preparative HPLC (MeOH/H_2O, 70:30 v/v) to yield physapubescin I (1.4 g). Physapubescin I (purity > 98.0%) was identified by comparing its ^1H and ^{13}C NMR spectroscopic data with those reported in the literature [29]. Physapubescin I was dissolved in DMSO to make a stock solution, aliquoted, and stored at −20 °C. The DMSO concentration was kept below 0.5% in all cell cultures used and did not exert any detectable effect on cell growth or death.

2.2. Molecular docking

Crystal structure of human KGA (PDB code: 3VP1) [9] was obtained from the Protein Data Bank. The docking was operated by ICM 3.7.3 modeling software on an Intel i7 4960 processor (MolSoft LLC, San Diego, CA). And ligand binding pocket residues were selected by graphical tools in ICM software to create the boundaries of docking search. The glutamate and BPTES were co-crystallized ligands in this crystal structure for docking, and they were deleted when setting up the receptor in docking calculation and potential energy maps of the receptor were calculated using default parameters. Compounds were input into ICM and an index file was created. Conformational sampling was based on the Monte Carlo procedure 30, and finally the lowest-energy and the most favorable orientation of the ligand were selected.

2.3. Cloning, expression, and purification of KGA

The catalytical domain of human KGA (cKGA) encoding amino acids 221–553 was cloned into pET26(b) vector with C-terminal His tag and expressed in *E. coli* BL21 (DE3)-RIL-Condon plus cells. The cells were cultured in LB media at 37 °C to OD value at 0.6–0.8, then induced with 0.4 mM IPTG at 16 °C for 16 h. Cells were harvested by centrifugation and sonicated in the lysis buffer containing 50 mM Hepes (pH 7.5), 500 mM NaCl, 5 mM imidazole, 10% glycerol, 1 mM DTT, 0.1% (v/v) Triton X-100, and 1 mM PMSF (Sigma-Aldrich USA). After centrifugation (22 000*g* × 30 min, 4 °C), the soluble fraction was bound to Ni-NTA resin (Qiagen), and washed with a buffer containing 20 mM imidazole, then eluted with a buffer containing 300 mM imidazole. The protein was further purified by using a Superdex-200 column (GE-health care, USA) in a buffer containing 20 mM Hepes (pH 7.5), 200 mM NaCl, 10% glycerol, and 3 mM DTT.

2.4. Assays for KGA enzyme inhibition

The KGA profiling assays were used to evaluate the compound-dependent inhibition of KGA *in vitro* catalytic assay [31]. The activity and inhibition of KGA were determined by measuring the production-NADH using a microplate reader. The enzyme activity was measured in 100 μL system. Reaction buffer containing 50 mM Tris-Acetate (pH 8.6), 0.15 M K_2HPO_4, 0.1 mg/mL bovine serum albumin (BSA), 0.25 mM EDTA, 1 mM DTT, 4 mM NAD, 10 mM glutamine, 1 unit of glutamate dehydrogenase (GDH) and inhibitor were added to each well in 96-well plates. Finally, the KGA enzyme was added to initiate the reaction at the final concentration of 1 μM. Generation of NADH was monitored by 340 nm absorbance at 37 °C for 20 min. The IC_{50} values were calculated by fitted regression equation using the Log plot (GraphPad Prism 6). Each value was represented with means ± SD of three independent tests, each with three replicates.

2.5. Microscale thermophoresis (MST) assay

Specific details were referenced to the method of binding affinity determination by microscale thermophoresis [32]. According to the manufacturer's instructions, KGA was labeled with the Monolith NT™ Protein Labeling Kit RED (Cat#L001). Labeled protein was diluted to 200 nM by the buffer containing 20 mM HEPES (pH 7.5) and 0.05% (v/v) Tween-20. Compound was diluted in a range of concentration steps

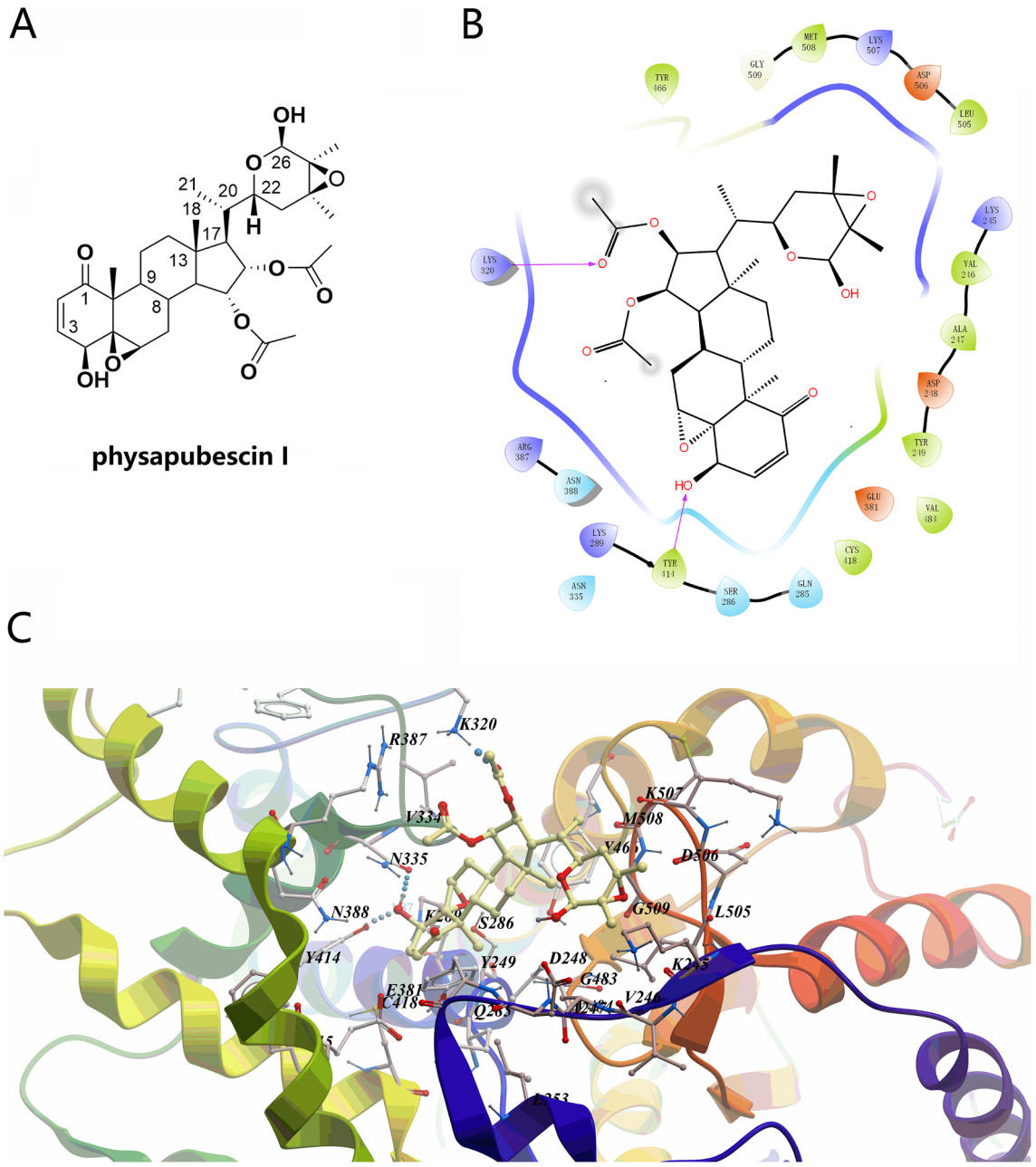

Fig. 1. The low-energy binding conformations of physapubescin I bound to KGA generated by virtual ligand docking. (A) The chemical structure of physapubescin I. (B) Ligand interaction diagram of physapubescin I with KGA. (C) The binding pocket analysis of physapubescin I on KGA.

and incubated with KGA for 10 min at room temperature. Samples were loaded into Monolith TM standard-treated capillaries, incubated for 10 min at 26 °C, then the thermophoresis was carried out on a Monolith NT.115 instrument (Nano Temper Technologies, München, Germany). Datas were obtained with 100% LED power and 20% MST. K_d value was fitted by using the NT Analysis software (Nano Temper Technologies, München, Germany).

2.6. Cell culture

The human pancreatic cancer cells (SW1990) and human fibrosarcoma cells (HT1080) were obtained from ATCC (Manassas, VA, USA) and cultured in Dulbecco's modified Eagle's medium (DMEM, Gibco BRL) supplemented with 10% (v/v) fetal bovine serum (FBS) (Invitrogen) and 1% (v/v) penicillin–streptomycin solution (Invitrogen). Cell culture was maintained in humidified atmosphere containing 5% CO_2 at 37 °C.

2.7. Cellular thermal shift assay (CETSA)

CETSA is a method based on the principle of ligand-induced stabilization of target proteins for direct detection of the ability of a compound binding to a target at the cellular level. Briefly, SW1990 cells cultured with 90% confluence in 100 × 20 mm tissue culture dishes were treated with media containing 0.2% DMSO or 20 μM physapubescin I (0.2% DMSO) for 12 h. After treatment, the cells were isolated with trypsin, collected by centrifugation, then resuspended in PBS. The cell suspension was divided equally into 5 PCR tubes and heated at a temperature gradient from 44 °C to 52 °C for 3 min. Subsequently, the cells were analyzed by a Western blot assay.

2.8. Western blot analysis

The harvested cells were lysed using liquid nitrogen and two repeated freeze-thaw cycles. Insoluble debris was removed by centrifugation and the concentration of protein was quantified using a BCA Protein Quantitation Kit (Beyotime, China). Equal amounts of protein (20–40 μg) from each sample were subjected to 10% SDS-PAGE and electrophoretically transferred to polyvinylidene difluoride membrane (PVDF) (Millipore, USA). After blocking for 2 h at room temperature with Tris-buffered saline containing 5% non-fat dry milk, the membrane was incubated overnight with the following primary antibodies: β-actin (A2228) and KGA (20170-1-AP). Protein bands were visualized using an enhanced chemiluminescence reagent (ECL Plus) (GE Healthcare, USA) after hybridization with a HRP conjugated secondary antibody. Band density was quantified using ImageJ software.

2.9. Cytotoxicity assay

The cells were seeded at a density of 5000 cells per well in 96-well plates and cultured overnight for cell attachment. Cells were incubated with different concentrations of physapubescin I (0–80 μM) for 48 h while BPTES and CB-839 were used as the positive control. Cell viability was then assessed using the CCK8 assay kit according to the manufacturer's instructions. Absorbance was measured at 450 nm using an enzyme-linked immunosorbent assay reader (Zeiss, OBSERVER D1/AX10 cam HRC). All experiments were performed in triplicate and the IC_{50} of physapubescin I was calculated from the dose response-inhibition curve by using GraphPad Prism 6.

2.10. siRNA transfection

Briefly, siRNA was designed and purchased from General Biosystems company. The SW1990 cells were transfected with 50 nM siKGA or siCtrl using Hieff Trans™ Liposomal Transfection reagent (YEASEN), according to the manufacturer's instructions. The sequences of siRNA1-3 and siCtrol are: GCAAAGAGCUGGUGGCCUCTTGAGGCC ACCAGCUCUUUGCTT; CUGAAUAUGUGCAUCGAUATTUAUCGAUGC ACAUAUUCAGTT; GAGGAAAGGUUGCAGAUUATTUAAUCUGCAACC UUUCCUCTT; UUCUCCGAACGUGUCACGUTTACGUGACACGUUCGGA GAATT. Subsequently, the cells were analyzed by a Western blot assay.

2.11. EdU and DAPI double staining to detect cell proliferation

The logarithmic growth phase cells were plated in 24-well plates at a density of 2×10^4–5×10^4 cells per well for 4–6 h. Then, cells were incubated in serum-free DMEM containing 50 μM EdU (RiboBio, Guangzhou, China) for 2 h, and treated with 5 μM, 10 μM physapubescin I or DMSO (negative control, all containing 0.2% DMSO). After 2 h, the medium was removed and cells were washed with PBS. Cells were fixed using fixing buffer (4% polyformaldehyde) for 30 min, then subjected to Apollo staining and DNA staining according to the manufacturer's instructions. Cells were imaged using a fluorescence microscopy, and experiments were repeated at least three times. The number of EDU positive cells and DAPI positive cells were counted. The EdU positive ratio was quantified to DAPI positive cells.

2.12. Hoechst 33258 staining to detect cell apoptosis

The cells were incubated with physapubescin I for 24 h, stained with Hoechst 33258 at 37 °C for 30 min, then captured with a fluorescence microscope, and experiments were repeated at least three times. Apoptotic cells showing fragmentation and dense staining of nuclei, and stained cells were counted. The rate of cells apoptosis was quantified by the ratio of cells with fragmented and densely stained nuclei to all cells.

2.13. Cell proliferation assay

SW1990 cells were seeded into 96-well plates at a density of 2×10^3 per well. Cell proliferation was assessed for 24 h, 48 h, 72 h, 96 h at 37 °C and measured the absorbance at 490 nm using MTT method. The experiment was performed in triplicate.

2.14. Measurement of intracellular metabolism level

NADPH/$NADP^+$ ratio were determined by using $NADP^+$/NADPH Quantification Colorimetric Kit (BioVision, #K347-100). The abundance of intracellular glutamine (KeyGen, Nanjing, China A124), glutamate (KeyGen, Nanjing, China A074), (BioVision, #K778), aspartate (BioVision, #K552), oxaloacetate (BioVision, #K659) and malate (BioVision, #K637) was determined by using quantification kits, according the manufacturer's instruction. Briefly, 5×10^6 cells (10 cm dishes) were collected during log-phase growth by cell scraper, homogenized in 0.2 mL of provided buffers (on ice), and centrifuged at 4 °C for 10 min at 13,000*g*. Supernatants were deproteinized using 10 K ultrafiltration tube (Millipore, USA), analyzed and compared to standard curves. The signals obtained were normalized to the protein concentration calculated upon processing a parallel 10 cm dish.

2.15. Antitumor efficacy of physapubescin I in xenograft mouse model

All animal experiments were conducted in accordance with the Guide for the Care and Use of Laboratory Animals of Tongji Medical College, Huazhong University of Science and Technology and approved by the Ethics Committee. CB-17/SCID mice (male, 4 weeks old) were purchased from Beijing HFK Bioscience CO., LTD (Beijing, China). SW1990 cells (3×10^6 cells) were inoculated subcutaneously (s.c.) into the left flank of each mouse. After palpable tumors developed, mice were randomly divided into six groups (n = 9 for each group) and treated daily by gavage of natural saline or 5 mg/kg physapubescin I (both containing 0.2% DMSO) for 15 days. The dose volume was 0.1 mL/10 g body weight and the weight of mice was recorded every three days. Meanwhile, the tumor volume was measured with a vernier caliper every three days and calculated by the following formula: $(A \times B^2)/2$, where A was length and B was width of the two-dimension tumor. After mice were sacrificed, tumor weight was measured. The inhibition ratio (%) was calculated using the following equation: $I\% = 100\% \times [W_{\text{tumor (natural saline)}} - W_{\text{tumor (treated)}}]/W_{\text{tumor (natural saline)}}$.

For histological examinations, specimens including livers, spleens, kidneys and pancreas were fixed in 4% paraformaldehyde for 24 h, and subsequently embedded in paraffin wax and cut in 5 μm. H&E staining was carried out on sections of these normal tissues. After being dewaxed and rehydrated, these sections were dipped into Mayer's hematoxylin for 5 min. Followed by rinsing with H_2O, the sections were stained with 1% eosin Y solution for 3 min. The sections were dehydrated with alcohol and xylene. Finally, a mounting medium was added before covering with a cover slip.

2.16. Statistical analysis

Statistical analysis of the data was performed using Graph Pad Prism 6.0 software. The data were expressed as the means ± SD. Values were analyzed using SPSS version 12.0 software by one-way analysis of variance (ANOVA), and $P < 0.05$ was considered statistically significant.

3. Results

3.1. Virtual ligand screening

In order to discover new KGA inhibitors, over 100 compounds including withanolides, flavonoids, and coumarins from *Physalis*

pubescens were screened in silico against the KGA model (PDB code: 3VP1) by using ICM 3.7.3 modeling software (MolSoft LLC, San Diego, CA) [33] The lowest-energy and the most favorable orientation of the ligand was selected, followed by enzymatic inhibition assay to find potential natural KGA inhibitors (Supplementary Table 1). The results predicted that physapubescin I (Fig. 1A) may have strong binding affinity to KGA with the very negative mfScores of −122.50 (Table 2). From the generated docking model, physapubescin I extended into the active site of the enzyme, it occupied the cavity both containing the substrate and product of the enzyme, completely hindering the entrance of binding site. Hydrogen bonds were predicted between the ester carbonyl group at C-16 and Lys320, as well as between hydroxyl group at C-4 with Asn335 and Tyr414. Also, physapubescin I formed several key hydrophobic interactions with Tyr249, V484, and Tyr466 (Fig. 1B and C). To compare binding modes of KGA inhibitors, co-crystal structures of DON (PDB code: 4O7D) [16], BPTES (PDB code: 3VP1) [9] and CB-839 (PDB code: 5HL1) [34] with KGA were overlapped with the docking result of physapubescin I (Supplementary Fig. 1). As shown in Supplementary Fig. 1, BPTES (orange) and CB-839 (blue) are bound in an allosteric pocket which was just close to the catalytic site of the enzyme, where they are interacting with the "gating loop" to regulate the enzyme activities [34]. DON (purple), the substrate analogue, was bound with the same catalytic site of glutamine (green).

3.2. In vitro enzyme inhibition assay

To confirm the inhibition of KGA by physapubescin I *in vitro*, an enzyme inhibition assay was performed. The result demonstrated that physapubescin I significantly inhibited the activity of KGA *in vitro* with IC_{50} of 7.02 ± 0.89 μM (Fig. 2A, Supplementary Table 1), similar to the positive control BPTES with IC_{50} of 8.37 ± 0.25 μM, but worse than CB-839 with IC_{50} of 0.97 ± 0.04 μM [35] (Table 2). On the other hand, using glutamine as a substrate, we performed a steady-state enzyme kinetics study of physapubescin I inhibiting KGA. The results indicated that physapubescin I exhibited a mixed-type inhibition with both non-competitive and competitive characteristics, for Km was increased and Vmax was decreased when the concentrations of physapubescin I raised (Fig. 2B–C and Table 1). This enzyme kinetics result was consistent with the above docking model in which physapubescin I occupied both the entrance of the substrate and its binding site. Also, the inhibition caused by physapubescin I was reversible, as shown in Fig. 2D, the increasing concentrations of the substrate glutamine from 10 mM to 40 mM could abrogate the inhibition by 40 μM physapubescin I.

Table 1
Kinetic studies of enzyme inhibition by physapubescin I on KGA with glutamine as the substrate.

C (physapubescin I, μM)	Control	5	10	20
Vmax (OD/min)	0.13	0.10	0.07	0.06
Km (mM)	0.96	1.69	2.40	3.31

3.3. High binding affinity of compound-protein

The equilibrium dissociation constant K_d is the most straightforward parameter reflecting binding strength of compounds with proteins. We employed the microscale thermophoresis (MST), a method based on the fluorescent behaviour of protein in diverse ligand concentrations during thermophoresis to investigate interactions of protein–protein or protein-small molecule, to assess the binding affinity of physapubescin I and KGA [32]. The K_d value of physapubescin I obtained on MST was 2.89 ± 0.10 μM, exhibiting its high binding affinity with KGA (Fig. 3A).

The cellular thermal shift assay (CETSA) based on the ligand

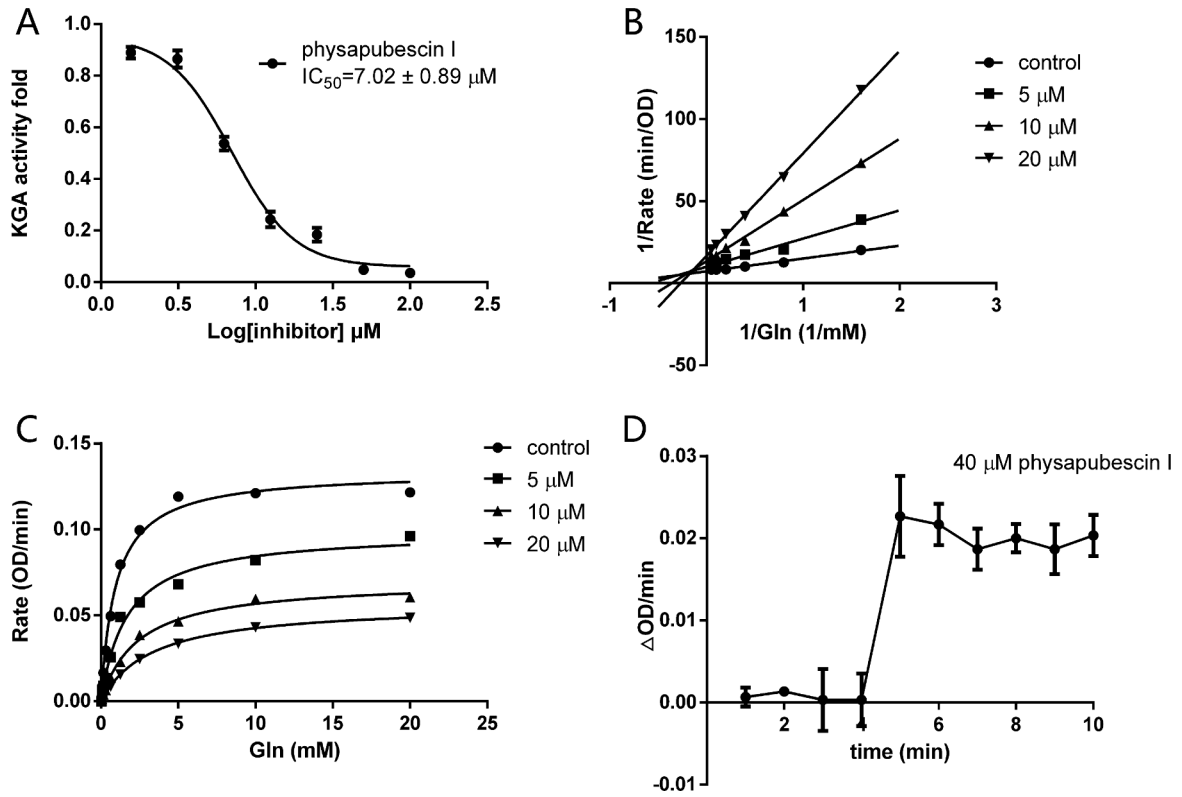

Fig. 2. *In vitro* enzyme inhibition assays. (A) Dose response inhibition of KGA activity by physapubescin I. (B) Line weaver-Burk double-reciprocal representation of the glutamine saturation profiles for KGA at a range of concentrations of physapubescin I. (C) Glutamine saturation profiles for KGA at a range of concentrations of physapubescin I. (D) Saturated inhibition assay. Glutamine was 10 mM at 1–4 min and increased to 40 mM at 4 min. Physapubescin I was 40 μM.

Table 2
Determination of physapubescin I about binding affinity, IC_{50} for enzyme and cells.

Compounds	mfScores[a] (kcal/mol)	K_d (μM)	IC_{50} (μM) for Enzyme	IC_{50} (μM) for Cells		
				SW1990	HT1080	MDA-MB-231
Physapubescin I	−122.50	2.89 ± 0.10	7.02 ± 0.89	3.34 ± 0.04	5.04 ± 0.05	2.06 ± 0.03
BPTES	–	–	8.37 ± 0.25[b]	35.33 ± 3.21	45.72 ± 4.67	25.20 ± 2.18
CB-839	–	–	0.97 ± 0.04[b]	13.06 ± 0.57[b]	–	–

"–"means no tested. "a" means Docking score/interaction potential of compounds with KGA (kcal/mol). "b" means this data is from reference [35].

induced stabilization of target proteins was employed to confirm the interaction between physapubescin I and KGA *in vitro*. The thermal stability of KGA in human pancreatic cancer cells SW1990 was tested at the temperature range of 44–52 °C. The KGA of 20 μM physapubescin I treated group was more thermostable than that of DMSO treated group, as the KGA band could still be clearly visible in higher temperature (Fig. 3B–C). These results implied that the specific binding of physapubescin I to KGA in SW1990 cells. The combination of MST and CETSA assays ensures precise assessment of KGA-physapubescin I binding strength and provides useful information for further studies.

3.4. Cytotoxicity assay of physapubescin I

Human pancreatic cancer cells SW1990, human fibrosarcoma cells HT1080 and human breast cancer cells MDA-MB-231 which exhibited highly dependence on glutamine [20,35], were employed to investigate proapoptosis activity and on-target activity of the KGA inhibitor. The growth inhibitory effects of physapubescin I against SW1990, HT1080 and MDA-MB-231 cells were investigated using CCK8 method. As a result, physapubescin I showed strong inhibitory effects toward SW1990, HT1080 and MDA-MB-231 cells with IC_{50} of 3.34 ± 0.04 μM, 5.04 ± 0.05 μM and 2.06 ± 0.03 μM, respectively (Fig. 4A–C), and was more potent than the known inhibitor BPTES, which has IC_{50} of 35.33 ± 3.21 μM, 45.72 ± 4.67 μM and 25.20 ± 2.18 μM against three cell lines, respectively (Table 2). The growth inhibitory effect of physapubescin I against SW1990 was better than CB-839, which has IC_{50} of 13.06 ± 0.57 μM [35].

3.5. siRNA knockdown of KGA

SW1990 cells transfected with siRNA1-3 down-regulated KGA expression compared to siRNA transfected control (si-Control) (Fig. 5A). SW1990 cells transfected with siRNA-2, siRNA-3 or si-Control were treated with physapubescin I. Then, the cell viability was analyzed. The results showed that knockdown of KGA by siRNA reduced the inhibition of physapubescin I to SW1990 cells (Fig. 5B).

3.6. Effects of physapubescin I on proliferation and proapoptosis of cells

We selected SW1990 cells for EdU and DAPI double staining assays to further determine the effect of physapubescin I on SW1990 cell proliferation. It was found that the number of EdU-positive cells treated with physapubescin I showed a significant dose-dependent decrease. And inhibitory effect of 10 μM physapubescin I was significantly stronger than that of 40 μM BPTES (Fig. 6A–B). These results demonstrated that physapubescin I could inhibit SW1990 cell proliferation more efficiently than the known KGA inhibitor, BPTES.

To verify whether physapubescin I has a pro-apoptotic effect on SW1990 and MDA-MB-231 cells, 5 μM and 10 μM physapubescin I, and 40 μM BPTES-treated cells were stained with Hoechst 33258, respectively. Compared with the control group, 5 μM and 10 μM physapubescin I treated cells obviously showed fragmentation and dense staining of nuclei, and that ratio was more than that of 40 μM BPTES treated cells (Fig. 6C–F). These results demonstrated that physapubescin I had a proapoptotic effect on SW1990 and MDA-MB-231 cells.

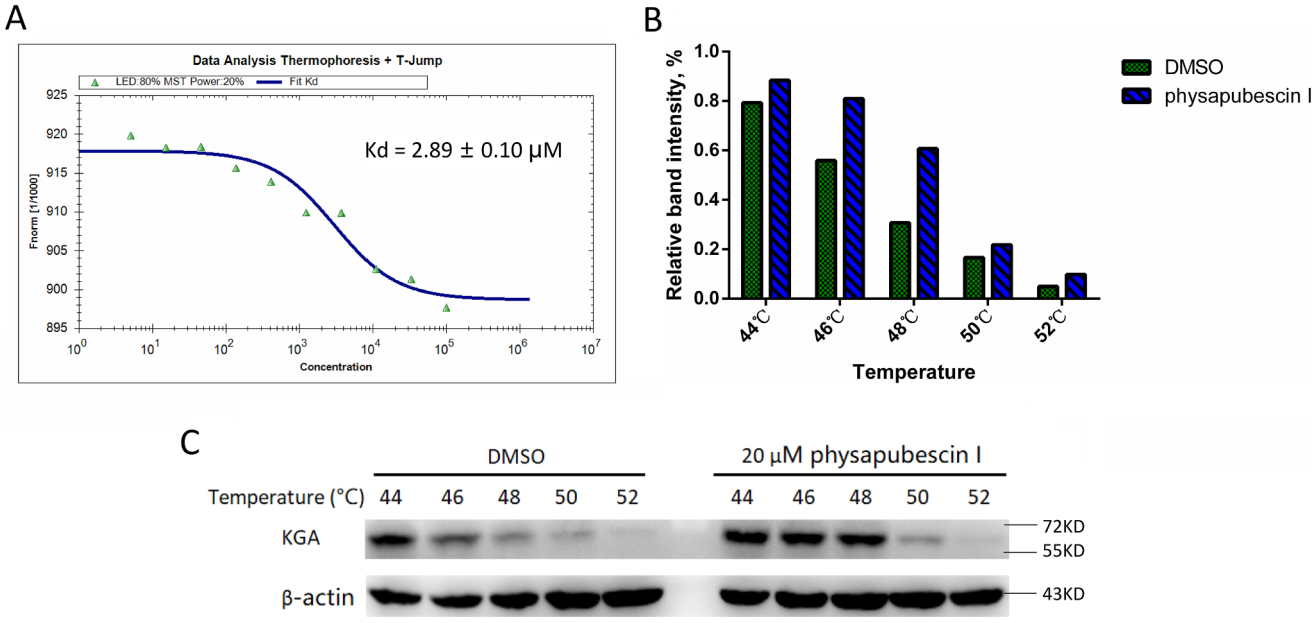

Fig. 3. Physapubescin I binding to KGA was confirmed by MST and CETSA asssays. (A) The binding curve of physapubescin I with KGA, K_d = 2.89 ± 0.10 μM in an independent experiment. (B) Quantification of band intensity of KGA in CETSA experiments in an independent experiment. (C) CETSA performed in SW1990 cells treated with 20 μM physapubescin I.

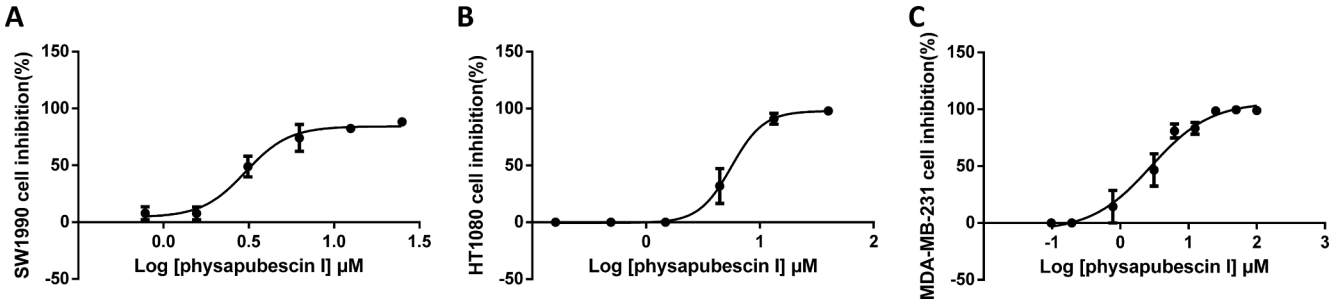

Fig. 4. Cell IC_{50} of physapubescin I. (A) The IC_{50} of physapubescin I to SW1990 cells was 3.34 ± 0.04 μM. (B) The IC_{50} of physapubescin I to HT1080 cells was 5.04 ± 0.05 μM. (C) The IC_{50} of physapubescin I to MDA-MB-231 cells was 2.06 ± 0.03 μM.

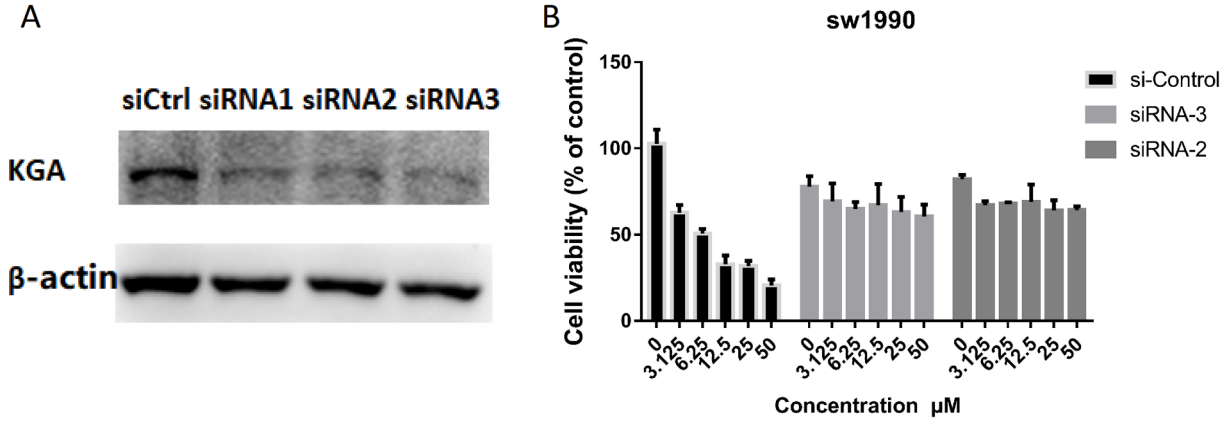

Fig. 5. Knockdown of KGA in SW1990 cells. (A) Knock down of KGA using siRNA in SW1990 cells followed by western blotting revealed the protein expression levels of KGA, compared with the mock siRNA-transfected control. (B) SW1990 cells were transfected with siRNA-2, siRNA-3 or si-Control followed by treatment with physapubescin I. Cell viability was analyzed.

3.7. Physapubescin I impaired glutamine metabolism

To further investigate whether the inhibitory effect of physapubescin I on SW1990 cell proliferation was mediated by inhibition of glutamine metabolism, a α-Ketoglutarate (α-KG) supplementing assay was carried out. The results showed that 5 μM physapubescin I significantly inhibited cell proliferation, while the addition of 16 mM α-KG relieved the inhibition of cell proliferation induced by physapubescin I. (Fig. 7A). These results indicated that the inhibitory effect of physapubescin I on SW1990 cell proliferation was closely related to glutamine metabolism.

On the other hand, the effects of different concentrations of physapubescin I on the intracellular glutamine and its downstream metabolites were studied in detail and compared with BPTES. The results showed that it could significantly reduce the consumption of glutamine in SW1990 cells and decrease the production of glutamate and its downstream metabolites including oxaloacetic acid, aspartate, and malate (Fig. 7B).

Likewise, physapubescin I significantly reduced the proportion of NADPH/$NADP^+$ in cells. These results indicated that physapubescin I impaired the glutamine metabolism, thereby reduced downstream products of tricarboxylic acid cycle which provided energy and participated in the synthesis of biological macromolecules, and consequently inhibited cell growth and proliferation. Therefore, physapubescin I reduced glutamine consumption in SW1990 cells, and correspondingly increased the intracellular level of glutamine, and decreased the level of glutamate and its downstream metabolites.

3.8. In vivo inhibitory effect of physapubescin I in SW1990 solid tumor

In this study, we employed SW1990 xenograft mouse model to evaluate the *in vivo* antineoplastic activities of physapubescin I. Results showed that intraperitoneal injection of 5 mg/kg physapubescin I could significantly inhibit the growth of the tumor ($P < 0.01$) (Fig. 8A, C and D). Examination of livers, spleens, kidneys and pancreas of mice treated with physapubescin I revealed no pathological changes in these normal tissues compared with the natural saline-treated group by H&E-stained assay (Fig. 8E). Furthermore, physapubescin I showed no effect on mice body weight (Fig. 8B), suggesting its low toxicities *in vivo*.

4. Discussion and conclusions

Kidney-type glutaminase (KGA), catalyzing the hydrolysis of glutamine to glutamate, plays a key role in cancer cells, where it is overexpressed and maintains cell survival by supplying energy through glutamine metabolism pathway [36–38]. KGA has been regarded as a new target for cancer therapy in recent years [39,40].

Efforts have been made to develop specific KGA inhibitors to improve their efficiency and specificity, and to reduce doses and side effects. Although KGA has been widely studied as a key metabolic enzyme, the numbers of its inhibitors found so far are relatively few. For example, DON, a traditional KGA inhibitor, is a valuable tool to explain the physiological effects of KGA, but its weak efficacy and lack of selectivity hinder its application as a therapeutic agent [18]. BPTES, another inhibitor, has been terminated in the preclinical stage due to its poor metabolic stability and low solubility [19,20]. CB-839 is now the only GLS inhibitor in phase I/II clinical trials and combined with other agents [20]. Since de novo design for new targeted antitumor drug is a difficult task, natural products and their derivatives are good alternatives to obtain active lead compounds.

Physalis pubescens is an edible and medical plant with a wide distribution in the world, and its nutritious and delicious fruits are a kind of popular healthy food. Here, we reported physapubescin I discovered from its fruits, husk tomato, as a truly natural KGA inhibitor

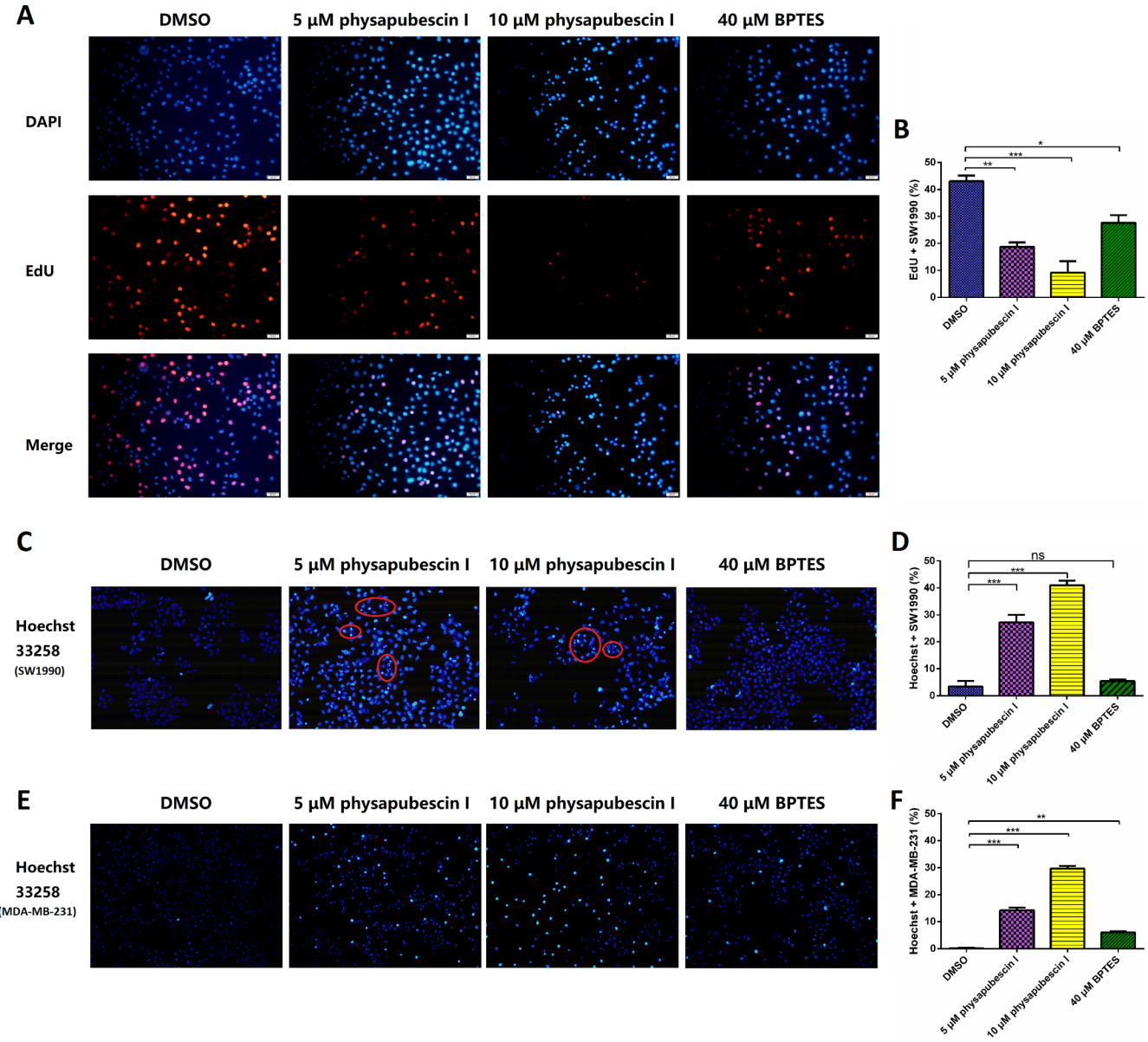

Fig. 6. Effects of physapubescin I on proliferation and proapoptosis of cells. (A) DAPI and EdU double staining was used to determine the effect of different concentrations of physapubescin I on the proliferation of SW1990 cells. BPTES was used as positive control. (B) The EdU positive ratio was quantified to DAPI positive cells. (C) Physapubescin I induced SW1990 cells apoptotic effect detected by Hoechst 33258 staining. The cells were treated with physapubescin I (5 μM and 10 μM) for 24 h, then stained with Hoechst 33,258 and observed through a fluorescence microscope (× 200 magnification). (D) The rate of SW1990 cells apoptosis was quantified by the ratio of cells with fragmented and densely stained nuclei to all cells. (E) Physapubescin I induced MDA-MB-231 cells apoptotic effect detected by Hoechst 33258 staining. (F) The rate of MDA-MB-231 cells apoptosis was quantified by the ratio of cells with fragmented and densely stained nuclei to all cells.

structurally distinct from BPTES. And the compound-KGA complex (3D model) further disclosed the molecular basis of physapubescin I targeting KGA and its kinetics mechanism, which was consistent with the results of MST, CETSA and enzyme inhibition assay. As reported in previous study that truncated KGA having the main catalytic domain had the same enzymatic activity as the full-length protein *in vitro* or cells [41], so it should not be an issue for the initial screen by using the truncated KGA protein in this study. As we further validate the results through cytotoxicity assays, siRNA transfection and CETSA experiments, all these were based on the full-length KGA protein. Furthermore, at the cellular level, physapubescin I showed stronger proapoptosis and anti-proliferation than BPTES against SW1990, MDA-MB-231 or HT1080 cells which exhibited highly dependence on glutamine, indicating that physapubescin I killed these specific cancer cell lines through a KGA dependent manner. Knockdown of KGA by siRNA reduced the inhibition of physapubescin I to SW1990 cells. Outcomes of cellular metabolite analysis also demonstrated that physapubescin I impaired glutamine metabolism to trigger mechanism-based cell death. Furthermore, physapubescin I showed a significant inhibition on the tumor growth in SW1990 xenograft mouse model with low toxicities, which suggested its potential therapeutic utilities in pancreatic cancer treatment.

Physapubescin I, a natural compound extracted from the husk tomato, has shown strong anti-tumor effects in the pancreatic cancer cell model and the murine xenograft model, with high targeting and low toxicities. Therefore, compared with known KGA inhibitors, physapubescin I has more significant values for further investigation. Our previous research reported that one withanolide, physapubescin K showed KGA inhibitory activity [35]. Herein, physapubescin I is also found to be another KGA inhibitor. Comparison of two withanolides showed the

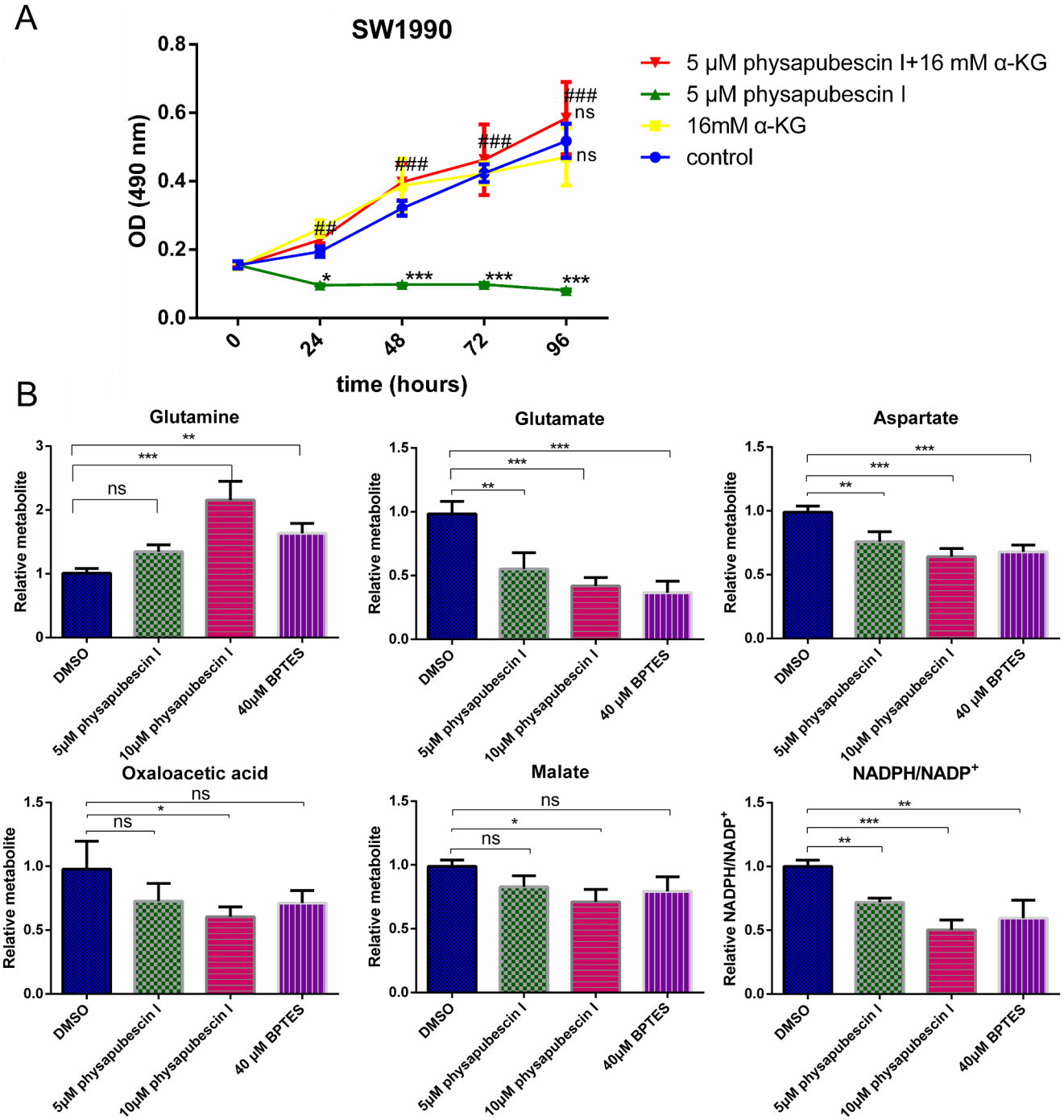

Fig. 7. Physapubescin I impaired glutamine metabolism in SW1990 cells. (A) The α-KG relieved the inhibition of cell proliferation by physapubescin I in SW1990 cells. The difference between control group and groups treated by 5 μM physapubescin I, 5 μM physapubescin I and 16 mM α-KG or 16 mM α-KG was indicated by *. The difference between groups treated with 5 μM physapubescin I or 5 μM physapubescin I and 16 mM α-KG was indicated by #. (B) Effects of physapubescin I on glutamine metabolism. Relative intracellular metabolite levels and NADPH/$NADP^+$ were measured in SW1990 cells treated with DMSO, 5 μM or 10 μM physapubescin I for 4 h. BPTES was used as a positive control. The treated and untreated conditions were compared by one-way analysis of variance. *$P < 0.05$; **$P < 0.01$; ***$P < 0.001$; ns means no significant difference.

similar structures, except for the presence of an acetoxyl group on C-16 and the absence of a methoxyl group on C-26 in physapubescin I. Our present research suggested that the KGA inhibition was related to the presence of functional groups (4β-hydroxy-2-en-1-one in ring A and 5β,6β-epoxy in ring B), but the substituent groups in ring D and the side chain were not critical for the activity of withanolides. The preliminary structure-activity relationship might provide reference for the further structural derivation of withanolides targeting at KGA. Indeed, some literatures report GAC is more active than KGA and overexpressed in many cancers, indicating that GLS1 alternative splicing may play an important role in the presumed higher glutaminolytic flux in cancers [20], but the role of physapubescin I for the GAC is unclear, which requires further study and validation. In future studies, we will further explore drug combinations, structural modifications based on KGA structure, and experimental therapies on other cancers.

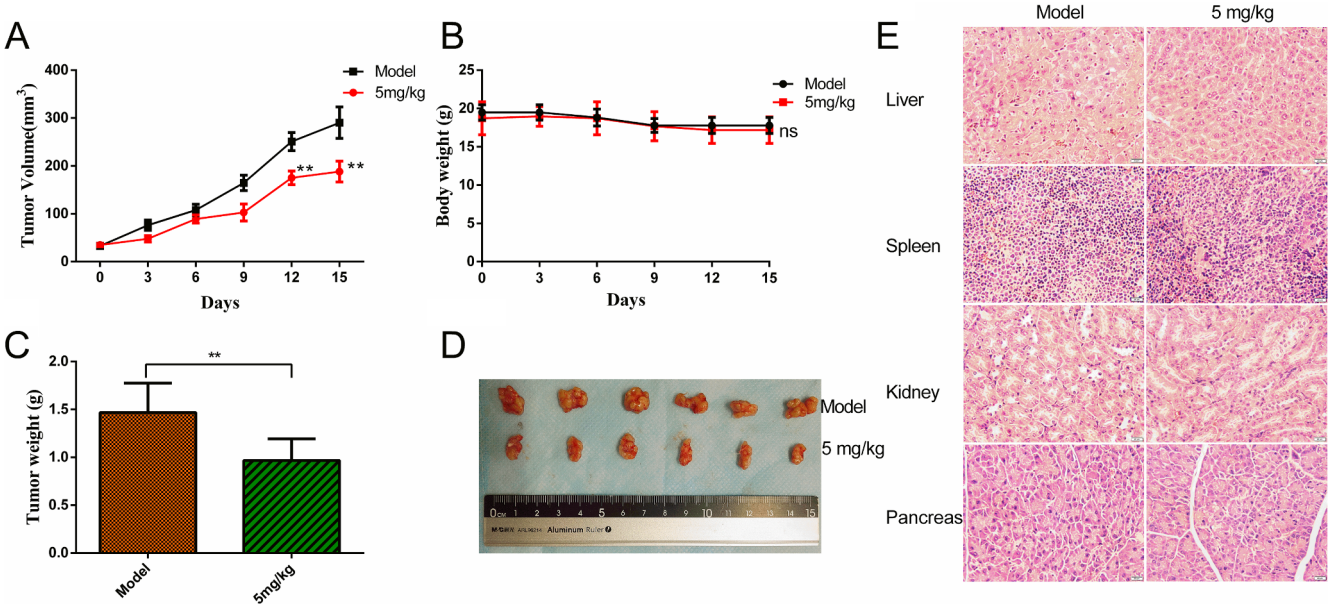

Fig. 8. Effects of physapubescin I on cancer cell growth in xenograft mouse models. (A) The average tumor volume decreased after treatment with 5 mg/kg physapubescin I compared with natural saline-treated group. (B) Physapubescin I showed no effect on mice body weight. (C) The average tumor weight decreased after treatment with 5 mg/kg physapubescin I, compared with natural saline-treated group. (D) After treatment for 2 weeks, differences in tumor size were observed. (E) Representative H&E-stained sections of livers, spleens, kidneys and pancreas. ** means $P < 0.01$.

Declaration of Competing Interest

The authors claim that the researchers in this study have no conflict of interest.

Acknowledgement

This work was supported by the National Natural Science Foundation of China (NSFC) (grant numbers 81773594, U1703111, U1803122, and 81773637), China; the Fundamental Research Fund for the Central Universities (grant number 2017KFYXJJ151), China; Liaoning Province Natural Science Foundation (grant number 2019-MS-299), China; Liaoning Innovative Talents Program of Higher Education Institutions (grant number LR2016002), China. We acknowledge support from Schrödinger Release 2018-4: Maestro, Schrödinger, LLC, New York, NY, 2018.

Appendix A. Supplementary material

Supplementary data to this article can be found online at https://doi.org/10.1016/j.bioorg.2019.103186.

References

[1] L. Cheng, C.R. Wu, L.H. Zhu, H. Li, L.X. Chen, Physapubescin, a natural withanolide as a kidney-type glutaminase (KGA) inhibitor, Bioorg. Med. Chem. Lett. 27 (5) (2017) 1243–1246.
[2] L. Xiang, J. Mou, B. Shao, Y. Wei, H. Liang, N. Takano, G.L. Semenza, G. Xie, Glutaminase 1 expression in colorectal cancer cells is induced by hypoxia and required for tumor growth, invasion, and metastatic colonization, Cell Death Dis. 10 (2) (2019) 40.
[3] S. Takahashi, J. Saegusa, S. Sendo, T. Okano, K. Akashi, Y. Irino, A. Morinobu, Glutaminase 1 plays a key role in the cell growth of fibroblast-like synoviocytes in rheumatoid arthritis, Arthritis. Res. Ther. 19 (1) (2017) 76.
[4] C. Lobo, M.A. Ruiz-Bellido, J.C. Aledo, J. Marquez, D.C.I. Nunez, F.J. Alonso, Inhibition of glutaminase expression by antisense mRNA decreases growth and tumourigenicity of tumour cells, Biochem. J. 348 (Pt 2) (2000) 257–261.
[5] B.J. Altman, Z.E. Stine, C.V. Dang, From Krebs to clinic: glutamine metabolism to cancer therapy, Nat. Rev. Cancer 16 (10) (2016) 619–634.
[6] Y. Li, J.W. Erickson, C.A. Stalnecker, W.P. Katt, Q. Huang, R.A. Cerione, S. Ramachandran, Mechanistic basis of glutaminase activation: a key enzyme that promotes glutamine metabolism in cancer cells, J. Biol. Chem. 291 (40) (2016) 20900–20910.
[7] C.T. Hensley, A.T. Wasti, R.J. DeBerardinis, Glutamine and cancer: cell biology, physiology, and clinical opportunities, J. Clin. Invest. 123 (9) (2013) 3678–3684.
[8] W.P. Katt, M.J. Lukey, R.A. Cerione, A tale of two glutaminases: homologous enzymes with distinct roles in tumorigenesis, Future Med. Chem. 9 (2) (2017) 223–243.
[9] K. Thangavelu, C.Q. Pan, T. Karlberg, G. Balaji, M. Uttamchandani, V. Suresh, H. Schuler, B.C. Low, J. Sivaraman, Structural basis for the allosteric inhibitory mechanism of human kidney-type glutaminase (KGA) and its regulation by Raf-Mek-Erk signaling in cancer cell metabolism, Proc. Natl. Acad. Sci. USA 109 (20) (2012) 7705–7710.
[10] D.R. Wise, R.J. DeBerardinis, A. Mancuso, N. Sayed, X.Y. Zhang, H.K. Pfeiffer, I. Nissim, E. Daikhin, M. Yudkoff, S.B. McMahon, C.B. Thompson, Myc regulates a transcriptional program that stimulates mitochondrial glutaminolysis and leads to glutamine addiction, Proc. Natl. Acad. Sci. USA 105 (48) (2008) 18782–18787.
[11] P. Gao, I. Tchernyshyov, T.C. Chang, Y.S. Lee, K. Kita, T. Ochi, K.I. Zeller, A.M. De Marzo, J.E. Van Eyk, J.T. Mendell, C.V. Dang, c-Myc suppression of miR-23a/b enhances mitochondrial glutaminase expression and glutamine metabolism, Nature 458 (7239) (2009) 762–765.
[12] X. Xu, J. Li, X. Sun, Y. Guo, D. Chu, L. Wei, X. Li, G. Yang, X. Liu, L. Yao, J. Zhang, L. Shen, Tumor suppressor NDRG2 inhibits glycolysis and glutaminolysis in colorectal cancer cells by repressing c-Myc expression, Oncotarget 6 (28) (2015) 26161–26176.
[13] J.B. Wang, J.W. Erickson, R. Fuji, S. Ramachandran, P. Gao, R. Dinavahi, K.F. Wilson, A.L. Ambrosio, S.M. Dias, C.V. Dang, R.A. Cerione, Targeting mitochondrial glutaminase activity inhibits oncogenic transformation, Cancer Cell 18 (3) (2010) 207–219.
[14] J. Lora, F.J. Alonso, J.A. Segura, C. Lobo, J. Marquez, J.M. Mates, Antisense glutaminase inhibition decreases glutathione antioxidant capacity and increases apoptosis in Ehrlich ascitic tumour cells, Eur. J. Biochem. 271 (21) (2004) 4298–4306.
[15] S. Ramachandran, C.Q. Pan, S.C. Zimmermann, B. Duvall, T. Tsukamoto, B.C. Low, J. Sivaraman, Structural basis for exploring the allosteric inhibition of human kidney type glutaminase, Oncotarget 7 (36) (2016) 57943–57954.
[16] K. Thangavelu, Q.Y. Chong, B.C. Low, J. Sivaraman, Structural basis for the active site inhibition mechanism of human kidney-type glutaminase (KGA), Sci. Rep. 4 (2014) 3827.
[17] D. Yu, X. Shi, G. Meng, J. Chen, C. Yan, Y. Jiang, J. Wei, Y. Ding, Kidney-type glutaminase (GLS1) is a biomarker for pathologic diagnosis and prognosis of hepatocellular carcinoma, Oncotarget 6 (10) (2015) 7619–7631.
[18] S.C. Zimmermann, B. Duvall, T. Tsukamoto, Recent progress in the discovery of allosteric inhibitors of kidney-type glutaminase, J. Med. Chem. 62 (1) (2019) 46–59.
[19] K. Shukla, D.V. Ferraris, A.G. Thomas, M. Stathis, B. Duvall, G. Delahanty, J. Alt, R. Rais, C. Rojas, P. Gao, Y. Xiang, C.V. Dang, B.S. Slusher, T. Tsukamoto, Design, synthesis, and pharmacological evaluation of bis-2-(5-phenylacetamido-1,2,4-thiadiazol-2-yl)ethyl sulfide 3 (BPTES) analogs as glutaminase inhibitors, J. Med. Chem. 55 (23) (2012) 10551–10563.
[20] X. Xu, Y. Meng, L. Li, P. Xu, J. Wang, Z. Li, J. Bian, Overview of the development of glutaminase inhibitors: achievements and future directions, J. Med. Chem. 62 (3) (2019) 1096–1115.

[21] R. Catane, D.D. Von Hoff, D.L. Glaubiger, F.M. Muggia, Azaserine, DON, and azotomycin: three diazo analogs of L-glutamine with clinical antitumor activity, Cancer Treat. Rep. 63 (6) (1979) 1033–1038.
[22] M. Song, S.H. Kim, C.Y. Im, H.J. Hwang, Recent development of small molecule glutaminase inhibitors, Curr. Top. Med. Chem. 18 (6) (2018) 432–443.
[23] Y. Sun, X. Feng, X. Liu, C. Qian, X. Che, F. Cao, S. Jin, D. Meng, Caudatan A, an undescribed human kidney-type glutaminase inhibitor with tetracyclic flavan from Ohwia caudata, Phytochemistry 152 (2018) 22–28.
[24] S.C. Zimmermann, E.F. Wolf, A. Luu, A.G. Thomas, M. Stathis, B. Poore, C. Nguyen, A. Le, C. Rojas, B.S. Slusher, T. Tsukamoto, Allosteric Glutaminase Inhibitors Based on a 1,4-Di(5-amino-1,3,4-thiadiazol-2-yl)butane Scaffold, ACS Med. Chem. Lett. 7 (5) (2016) 520–524.
[25] L. Ji, Y. Yuan, Z. Ma, Z. Chen, L. Gan, X. Ma, D. Huang, Induction of quinone reductase (QR) by withanolides isolated from Physalis pubescens L. (Solanaceae), Steroids 78 (9) (2013) 860–865.
[26] L. Xu, R.X. Wang, Y.Y. Yang, B. Wang, Studies on medicinal plants of the genus Physalis China resources, Zhongguoyeshengzhiwuziyuan 28 (01) (2009) 21–23.
[27] L.X. Chen, H. He, F. Qiu, Natural withanolides: an overview, Nat. Prod. Rep. 28 (4) (2011) 705–740.
[28] L.X. Chen, G.Y. Xia, H. He, J. Huang, F. Qiu, X.L. Zi, New withanolides with TRAIL-sensitizing effect from Physalis pubescens L, RSC Adv. 6 (58) (2016) 52925–52936.
[29] G. Xia, Y. Li, J. Sun, L. Wang, X. Tang, B. Lin, N. Kang, J. Huang, L. Chen, F. Qiu, Withanolides from the stems and leaves of Physalis pubescens and their cytotoxic activity, Steroids 115 (2016) 136–146.
[30] D.J. Newman, G.M. Cragg, Natural products as sources of new drugs from 1981 to 2014, J Nat Prod 79 (3) (2016) 629–661.
[31] M.I. Gross, S.D. Demo, J.B. Dennison, L. Chen, T. Chernov-Rogan, B. Goyal, J.R. Janes, G.J. Laidig, E.R. Lewis, J. Li, A.L. Mackinnon, F. Parlati, M.L. Rodriguez, P.J. Shwonek, E.B. Sjogren, T.F. Stanton, T. Wang, J. Yang, F. Zhao, M.K. Bennett, Antitumor activity of the glutaminase inhibitor CB-839 in triple-negative breast cancer, Mol. Cancer Ther. 13 (4) (2014) 890–901.
[32] L. Khavrutskii, J. Yeh, O. Timofeeva, S.G. Tarasov, S. Pritt, K. Stefanisko, N. Tarasova, Protein purification-free method of binding affinity determination by microscale thermophoresis, J. Vis. Exp. (78) (2013) e50541.
[33] R. Abagyan, M. Totrov, D. Kuznetsov, ICM-A new method for protein modeling and design: applications to docking and structure prediction from the distorted native conformation, J. Comput. Chem. 15 (5) (1994) 488–506.
[34] Q. Huang, C. Stalnecker, C. Zhang, L.A. McDermott, P. Iyer, J. O'Neill, S. Reimer, R.A. Cerione, W.P. Katt, Characterization of the interactions of potent allosteric inhibitors with glutaminase C, a key enzyme in cancer cell glutamine metabolism, J. Biol. Chem. 293 (10) (2018) 3535–3545.
[35] C. Wu, M. Zheng, S. Gao, S. Luan, L. Cheng, L. Wang, J. Li, L. Chen, H. Li, A natural inhibitor of kidney-type glutaminase: a withanolide from Physalis pubescens with potent anti-tumor activity, Oncotarget 8 (69) (2017) 113516–113530.
[36] J.W. Erickson, R.A. Cerione, Glutaminase: a hot spot for regulation of cancer cell metabolism? Oncotarget 1 (8) (2010) 734–740.
[37] R.J. DeBerardinis, T. Cheng, Q's next: the diverse functions of glutamine in metabolism, cell biology and cancer, Oncogene 29 (3) (2010) 313–324.
[38] J. Son, C.A. Lyssiotis, H. Ying, X. Wang, S. Hua, M. Ligorio, R.M. Perera, C.R. Ferrone, E. Mullarky, N. Shyh-Chang, Y. Kang, J.B. Fleming, N. Bardeesy, J.M. Asara, M.C. Haigis, R.A. DePinho, L.C. Cantley, A.C. Kimmelman, Glutamine supports pancreatic cancer growth through a KRAS-regulated metabolic pathway, Nature 496 (7443) (2013) 101–105.
[39] M.J. Seltzer, B.D. Bennett, A.D. Joshi, P. Gao, A.G. Thomas, D.V. Ferraris, T. Tsukamoto, C.J. Rojas, B.S. Slusher, J.D. Rabinowitz, C.V. Dang, G.J. Riggins, Inhibition of glutaminase preferentially slows growth of glioma cells with mutant IDH1, Cancer Res. 70 (22) (2010) 8981–8987.
[40] A.P. van den Heuvel, J. Jing, R.F. Wooster, K.E. Bachman, Analysis of glutamine dependency in non-small cell lung cancer: GLS1 splice variant GAC is essential for cancer cell growth, Cancer Biol. Ther. 13 (12) (2012) 1185–1194.
[41] Y. Li, J. Peer, R. Zhao, Y. Xu, B. Wu, Y. Wang, C. Tian, Y. Huang, J. Zheng, Serial deletion reveals structural basis and stability for the core enzyme activity of human glutaminase 1 isoforms: relevance to excitotoxic neurodegeneration, Transl. Neurodegener. (2017), https://doi.org/10.1186/s40035-017-0080-x.